High-Resolution Nanophotolithography in Atomic Force Microscopy Contact Mode

Yann Gilbert,* Radouane Fikri, Anna Ruymantseva, Gilles Lerondel, Renaud Bachelot, Dominique Barchiesi, and Pascal Royer

Laboratoire de Nanotechnologie et d'Instrumentation Optique, Université de Technologie de Troyes, Centre National de la Recherche Scientifique, B.P. 2060, 10010 Troyes Cedex, France

Received September 24, 2003; Revised Manuscript Received January 13, 2004

ABSTRACT: According to near field theory, when irradiated in specific conditions, a metallic tip can give rise to a field enhancement (FE) at its apex and then be used as a nanosource to illuminate a photosensitive sample. In the case of polymers containing azobenzene groups, this exaltation process can lead to a displacement and rearrangement of chromophores in the vicinity of the tip. Contact mode atomic force microscopy (AFM) has been chosen to observe the photoinduced pattern. The use of semiconductor and dielectric probes as well as a normal incidence illumination mode, which minimizes the field enhancement (FE), still induces nanopatterns whatever the polarization state of the actinic light. In these conditions, the adhesion forces appear to be mainly responsible for the nanopattern process. The residual solvent contained in the bulk acts as a plasticizer. The height of the photoinduced nanoprotrusion can be modulated by adjusting the vertical deflection of the tip. Photoinduced nanopatterning obtained in AFM contact mode appears as a new and easy technique of high-resolution nanophotolithography.

1. Introduction

The incorporation of photochromic molecules in an organic matrix leads to the formation of photosensitive materials whose properties can be changed after exposure to actinic light. The azobenzene group is well-known to present a structure that allows a trans−cis isomerization when it is exposed to an actinic light. Hartley was the first to show the existence of a cis isomer and propose the photoisomerization mechanism in 1937.[1]

In 1995, the experiments of Rochon et al.[2] and Kim et al.[3] proved that a macroscopic reorganization of photoresponsive organic molecules containing an azobenzene group can be induced when the sample is irradiated under specific conditions. Since this discovery, many experiments have been carried out in order to understand how a mechanism, which occurs at the angstrom scale, can generate a displacement of material at a macroscopic scale. Numerous researches have been carried out in far field in order to understand theoretically[4−9] and experimentally[10−20] the formation and the dynamics of photoinduced surface relief gratings (SRG).

The properties of the photochromic group depend on several factors, e.g., the way the azobenzene groups are incorporated into the matrix (grafted laterally on the chain or simply as a dopant) and the presence of electron acceptor and donor groups around the azobenzene chain. Only one azobenzene derived denominated by disperse red 1 (DR1) will be mentioned in this article. It belongs to the pseudo-stilbene class. This mesogenic group can be employed in a huge range of applications such as telecommunications in order to replace opto-electrical-opto conversion as well as holographic applications and optical data storage. This last point of application is developed in our laboratory that is focused on the near field optics via the use of apertureless scanning near field microscopy (ASNOM) and its applications (e.g., local excitation of fluorescent molecules).[21]

A promising application of ASNOM is the near field photolithography that consists of irradiating a sample of photochromic polymer (e.g., pseudo-stilbene azobenzene and azobenzene are considered like self-developing photosensitive photopolymers) under the vicinity of a metallic probe/tip mounted on an atomic force microscope (AFM).[19,22] Under specific conditions of irradiation, the confinement of the electromagnetic waves at the apex of the tip makes the probe act like a nanosource: an optical tip field enhancement (FE) so-called lightning rod effect occurs.[23,24] Therefore, the FE is diffracted from the apex of the tip on the surface of the polymer. Such an effect can be at the origin of a local three-dimensional reorganization of the photochromic polymer leading to the formation of a protrusion at the surface sample with a subwavelength resolution (it presents a lateral resolution of 50 nm on average). As it has been shown, this process can be carried out either in SNOM[26,28] or in ASNOM.[25,27] The topographic deformation is supposed to represent a snapshot of the FE. An indirect measure of an optical process could be then carried out by scanning the sample surface via the use of a commercial AFM. The efficiency and the "low cost" of fabrication (no new or complex technique needs to be employed in industrial field) tend to focus our attention to this process. Moreover, a better understanding and control of the mechanisms involved in the nanoprotrusion formation are needed complementary to the work already carried out on the tip effect via the AFM intermittent contact scanning mode. At last, one of the approaches developed in this article is to correlate results obtained in far field and near field.

In section 2, we will describe the experimental conditions including the preparation of the azo sample, the list of the optical equipments, and the illumination configurations. Section 3 will be divided into three main

* To whom correspondence should be addressed. E-mail: gilberty@utt.fr.

10.1021/ma035437g CCC: $27.50
Published on Web 04/22/2004

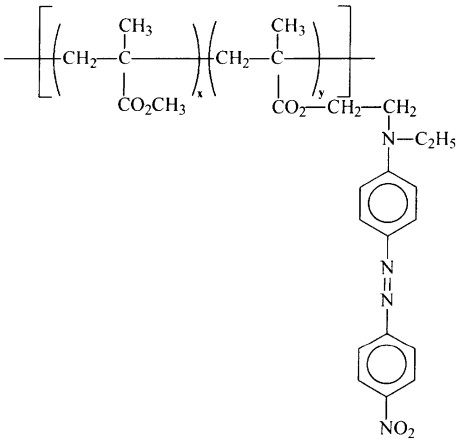

Figure 1. Chemical structure of the MMA-*co*-MDR1 copolymer.

parts: in the first part, after a brief review of the optical origin of the surface deformation, we analyze the dynamics of the nanopattern formation. Thus, the second part consists of measuring the influence of the electromagnetic singularity on the nanoprotrusion by modulating a few parameters in charge of the tip effect. Finally, the influence of the adhesion force is demonstrated in the last part, and a hypothesis on factors involved in the induction and growth of the nanoprotrusion is proposed.

2. Materials and Methods

2.a. Sample Preparation. The thin film used in the experiments is a copolymer composed of methyl methacrylate (MMA) units (forming the main chain) and DR1 grafted to a methacrylate unit by an appropriate spacer (see Figure 1.). MMA-*co*-MDR1 copolymer (70% MMA/30% MDR1) has been synthesized by Specific Polymers (its index of refraction can vary from 1.49 and 1.51). The copolymer is dissolved in filtered methyl isobutyl ketone (MIBK) which is a good polar solvent. After a complete dissolution, the copolymer is spin-coated onto clean glass slides for a microscope. The sample is then heated for few hours (depending on the concentration of the copolymer and the settings of the spin-coater) at a temperature of 120 °C. After such a thermal treatment, only a residual amount of solvent can be still present in the bulk.

The thickness is estimated to be 50 nm for thin samples and 150 nm for thick samples. Its root-mean-squared (rms) roughness is less than 2 nm when scanning a zone of 2 μm × 2 μm of the sample surface by AFM.

2.b. Experimental Protocol. The method can be divided into three steps: (1) approach of the probe (AFM tip) to the surface of the polymer in order to be in contact; (2) irradiation of the zone that is present at the vicinity of the tip by an actinic light; (3) topographic scan of the illuminated zone. Each step requires specific scientific instruments. The next subsections are focused on the descriptions of these instruments.

2.c. Scanning System: Probe Microscope. A M5 autoprobe commercial AFM from Parks Scientific Instrument scans the sample after the irradiation step. The scan mode chosen is the contact one. This mode was chosen because the nanopattern formation mechanism requires a better understanding of the interaction nature existing between polymers and the metallic tip. Moreover, few researches are carried out concerning the writing process of photochromic materials in contact mode. To the best of our knowledge, only Iwata et al.[27] induced nanometric modifications using the contact mode.

To avoid a mechanical nanoindentation, a nonconventional contact mode is used. The set point corresponding to the reference value assigned to the Z piezo of the scan master is adjusted in order to reach a value corroborating the retraction limit of the tip from the sample surface. This protocol is applied before any irradiation of the sample. For most of the experiments, the value of the set point is maintained constant during the illumination phase. We have to mention that the selected set point value can present variations according to the homogeneity of the studied area of the sample and/or according to the tribological properties of different samples due to their preparations (e.g., rigidity).

2.d. Optical Setup. The optical source is a CW frequency-doubled solid-state Nd:YAG pumped by diodes laser giving out a power (P) of 8 mW at $\lambda = 532$ nm with a Gaussian shape intensity distribution and a linear polarization. The emission wavelength of the actinic light is included in the absorption spectrum of the sample. (It corresponds simultaneously to the $\pi-\pi^*$ electronic transition in the case of trans isomer and to the $n-\pi^*$ transition in the case of cis isomer.)

An integrating sphere linked to a Powermeter from Melles Griot measures the power issued from the system. This power can be adjusted by an attenuator (index gradient film).

To module and to control the polarization precisely, a transverse field modulator (TFM) from Lasermetrics, an analogue of Pockels cells, is used. Its calibration requires a polarizer and an analyzer which is removed before the irradiation phase. A mechanical shutter controls the exposure time, and a lens, which focuses the beam on the surface, gives rise to a radius of the spot of 100 μm.

The sample is mainly positioning on a Dove prism (index of refraction 1.5). An adaptive liquid of refraction index of 1.5 is added between the prism and the microscope slide to facilitate the adherence of the sample on the prism and to avoid parasite reflections.

2.e. Illumination Mode. Three configuration modes have been selected to irradiate the sample; each mode offers advantages that will be developed (see Figure 2):

2.e.1. Reflection Mode. In this mode (see Figure 2a), the laser beam directly irradiates the tip (apex and its edges) and the sample. Then the modification of the surface topography gives rise to two kinds patterns in this configuration. Interaction of the actinic light and the light diffracted by the tip leads to the formation of interference patterns which have been already observed by H'Dhili et al.[25] We assume these fringes represent the optical far field.

In addition to the micron scale reorganization, a local protrusion under the tip apex appears with a mesoscopic subwavelength resolution. Many scientists interpret topographic modifications as a snapshot of the electromagnetic waves exaltation scattered by the apex of the metallic tip. Consequently, near field and "far field" patterns are both present and can be easily distinguished by probing the surface topography by AFM (see Figure 3).

2.e.2. Attenuated Total Reflection (ATR) Mode. The surface of the sample is illuminated via the prism of Dove. The incidence angle of the beam under the tip apex at the interface polymer/air must be equivalent to the total reflection critical angle. In this mode (see Figure 2b), only the apex of the tip is irradiated by the evanescent waves issued from the total reflection. Light diffracted and enhanced by the tip modifies the photosensitive sample in the vicinity of the apex only (see Figure 4), which decreases the aptitude of the far field pattern.

2.e.3. Normal Incidence Mode. As is shown in Figure 2c, the beam passes through the sample from its bottom. Consequently, this illumination mode requires the replacement of the prism by a beam splitter cube. Simulations based on the finite elements method (FEM) indicate that a transverse magnetic (TM) (or transverse electric (TE)) fundamental Gaussian mode beam propagating parallel to the tip tends to minimize the electromagnetic singularity of the probe. Therefore, this mode of illumination was chosen to indirectly evaluate the importance of the optical tip field enhancement in the nanopattern formation.

2.f. Probes. Two types of commercial tips from NTMDT operating in contact mode have been mainly used: tips CSC11 made of silicon and tips CSC17/Pt made of silicon coated by platinum. These tips have a radius of curvature lower than 35 nm and a full cone angle of less than 20°. Another kind of

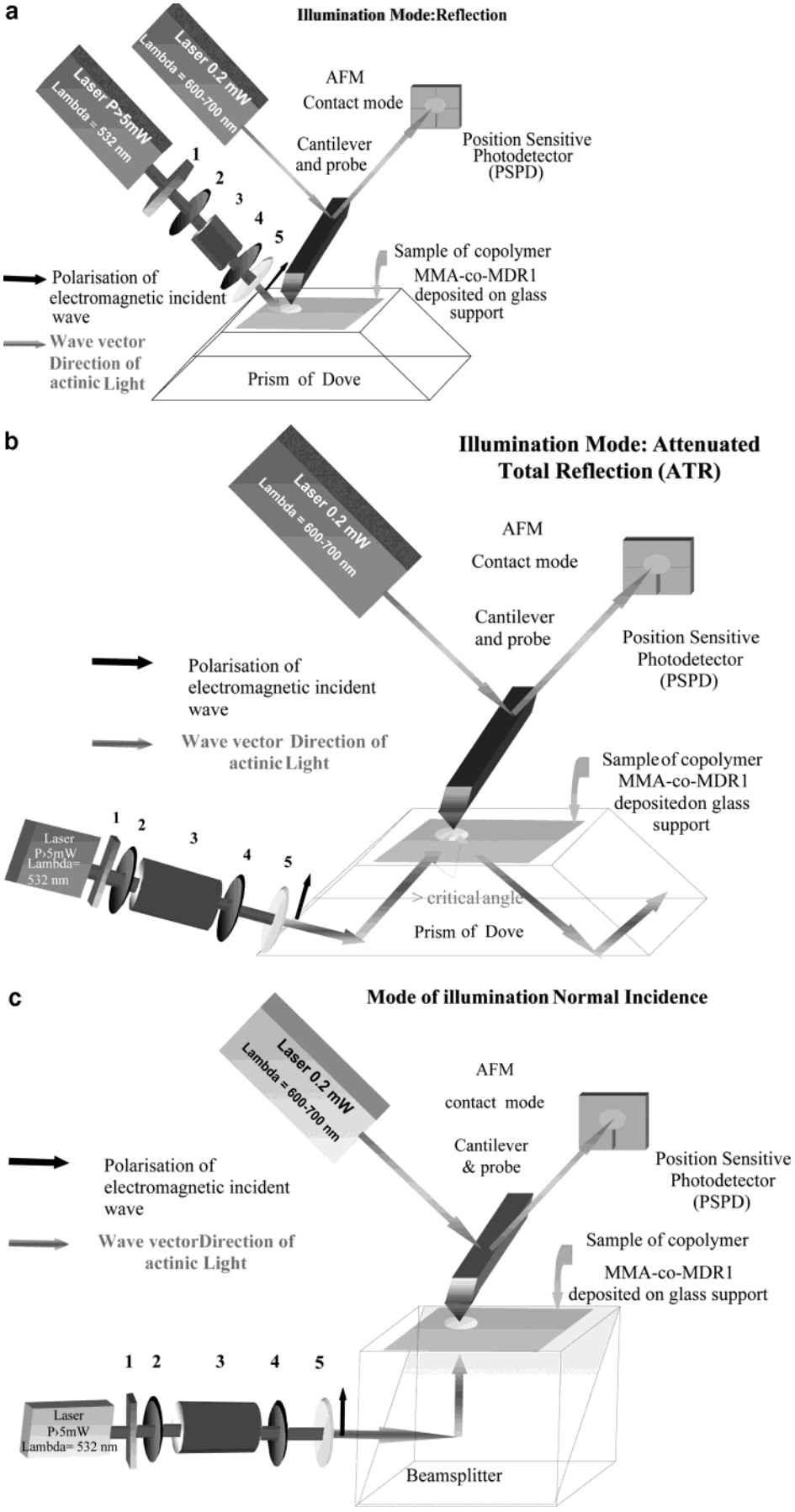

Figure 2. (a, top) Reflection experimental illumination configuration and representation of the interaction forces involved in the dot formation. (b, middle) Attenuated total reflection illumination configuration. (c, bottom) Normal incidence illumination configuration. 1, Shutter; 2, polarizer; 3, transverse field modulator (TFM); 4, analyzer (removed for irradiation process); 5, lens.

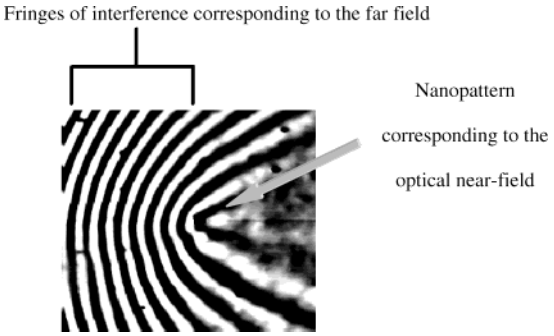

Figure 3. Topographic image of the pattern and fringes of interference (8 μm × 8 μm) obtained by illuminating the sample for 10 s at 532 nm in reflection illumination mode.

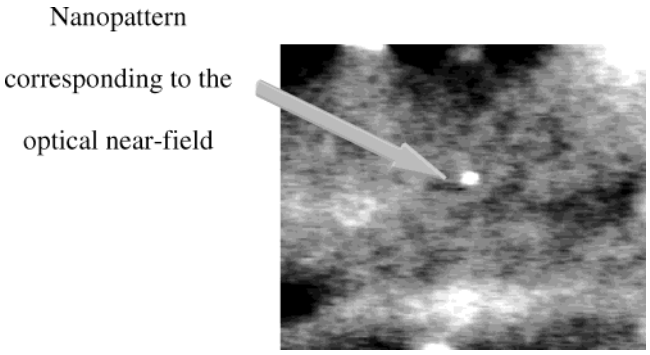

Figure 4. Topographic image of the pattern (2 μm × 2 μm) obtained by illuminating the sample for s at 532 nm in ATR illumination mode.

tips from NTMDT has been also used: the CSC 05/Al whisker tip. For this kind of tip, the radius of curvature is lower than 20 nm and the full cone angle is lower than 12°. To verify the influence of the tip field enhancement at the apex of the tip, the 0.6 μm sharp microlever Si_3N_4 dielectric tips from Park Scientific.

Instruments with large radius of curvature of 40 nm have been also used. The profile of each tip apex was checked by means of a scanning electron microscope (SEM) before and after utilization.

3. Results and Discussion

3.a. Photoinduced Process. The first experiments consist of verifying the optical origin of the nanoprotrusion induced in contact mode. Two factors may be also involved in this formation: the tip mechanical vibrations that may induce a nanoindentation and the heat diffusion from the metallic tip. The impact of the first parameter has been easily ruled out by completing the experimental protocol but without any light source. The aperture of the mechanical shutter was modulated as a function of time ($^1/_2$, 1, and 2 s). In this configuration, neither a nanoprotrusion nor nanometric cracking was observed in the vicinity of the tip. As a consequence, the mechanical factors are not in charge of the protrusion process in the absence of actinic light.

The influence of the heat diffusion form the tip can be demonstrated by heating a metallic tip (platinum tip CSC17) with a red He−Ne laser which does not allow one photon absorption of the trans isomer of the pseudostilbene copolymer (P = 2 mW, λ = 632.8 nm, exposure time = 45 s). In this case no modification of the surface was observed and this whatever the exposure time. Heat delivered by the tip cannot trigger the change of the sample surface potential. This result confirms the theoretical feature of azobenzene photoisomerization process. Heat diffusion from the tip does not seem to be involved in the triggering of the nanopatterning process.

These two simple experiments confirm the photoinduced nature of the nanoprotrusion formation and thus corroborate the results obtained in near field with the optical origin of patterns obtained in far field. The dot requires a local irradiation under the apex of the tip to be materialized. The next subsection is focused on the kinetic of the azo copolymer.

3.b. Dynamics of the Nanoprotrusion Growth. 3.b.1. Speed of the Chromophores Reorganization. For the pseudostilbene group, the $\pi-\pi^*$ absorption band of the trans isomer is quasi-superposed to the $n-\pi^*$ absorption band of the cis isomer. Therefore, the actinic light both activates a trans to cis and a cis to trans isomerization. There is also an inversion of the two absorption bands (compare to the first group of azobenzene) that shortens the cis isomer lifetime (in term of seconds). When the laser is turned off, a back-relaxation (cis to trans isomer) occurs. Moreover, this late relaxation modifies the mutual interaction between chromophores once illuminated. It is necessary to first determine the time required to fabricate a nanopattern to establish the influence of such relaxation effect on the pattern formation and on its stability.

The experimental procedure consists of irradiating the sample according to the illumination ATR mode (p polarization, P = 8 mW) with a whisker tip. A mechanical shutter controls the aperture time from 2 to 1/30 s. The spatial reorganization of chromophores gives rise to the induction of protrusions that are even observable after an irradiation time of 1/30 s. In this case, the fabricated nanopattern has a height of 1 nm dot and a full width at half-maximum (fwhm) of 45 nm. Obviously, when exposed with a more powerful actinic light, protrusion appears faster. Therefore, a dot with similar topographic features could be observed for a shorten exposure time. The reorganization of the photosensitive molecules appears to be a relatively fast process despite the intrinsic relaxation drawback.

This brief set of experiences leads to focalize our attention on the dynamic of the surface modulation and on the factors involved during the initialization and the nanopattern growth phases.

3.b.2. Effect of the Illumination Dose. In this subsection, the studied parameter is the variation of the nanopattern height resulting from the tridimensional chromophores reorganization under irradiation. The power of the laser is adjusted by the use of an attenuator film with a density gradient. Every selected zone is only irradiated once.

The following experiences involve the reflection illumination mode (see Figures 2a and 3) and a set point value maintained constant. The dynamic of the nanopattern growth is analyzed by modifications of two parameters: the incident illumination power (expressed in W cm^{-2}) and the sample irradiation time (expressed in seconds). These two parameters are adjusted independently. Therefore, the height of the dot is determined according to the illumination dose expressed in J cm^{-2} (power of illumination × exposure time). The curve shown in Figure 5 shows the influence of the illumination dose on the pattern height. The curve is similar to a saturation curve. For an energy dose lower than 7 J cm^{-2} the dot height is roughly proportional to the energy dose received. Over this value, the nanopattern height

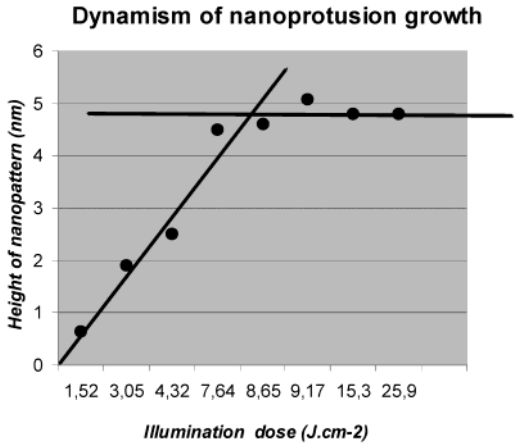

Figure 5. Nanopattern height (in nm) as a function of the energy dose received (J cm^{-2}). It shows two regimes: the growth is linear for doses less than a value corresponding to 7 J cm^{-2}. Over this illumination dose value, a saturation occurs. The dot formation presents the same dynamic either for ATR and reflections configurations.

tends to saturate. These results lead to analyze the dynamics of the nanopattern formation for values lower than 7 J cm^{-2} (assimilated to a threshold).

3.b.3. Reorganization of the Chromophores below the Threshold. To efficiently determine the dynamics of the nanopattern growth, an energy dose below the threshold of 7 J cm^{-2} has been used in combination with the reflection and ATR illumination modes (see Figure 2a,b). The results are presented in parts a−d of Figure 6, which show the AFM profiles of the dot obtained after an illumination time of 1, 2, 4, and 10 s, respectively. The dot formation seems to be divided into two different steps: (1) an angular depletion that appears under the tip with the formation of lateral lobes; (2) a progressive reduction of the depletion zone and the growth of the dot. The depletion occurs in the vicinity of the tip when the actinic light starts irradiating the surface. Migration of chromophores is induced in this zone, which leads to a photoinduced nanoindentation. This mechanism is clearly observed in the case of a thick sample featuring a homogeneous surface. Otherwise, in the case of thin samples, only a nanoprotrusion with a height of at least 1 nm can be observed without noticeable nanoindentation.

Two hypothesis are proposed to interpret this result: (1) The field enhancement at the apex of the tip could be in charge of this local depletion of matter. This process is similar to the one involved in the gratings formation which is due to the angular hole burning (AHB) and the angular redistribution (AR) mechanisms.[29] When the local illumination power is higher or equivalent to the value mentioned by Bian et al.,[12] this process would give rise to the formation of an irreversible nanoprotrusion under the tip. (2) The electromagnetic singularity would have a minor impact in the process, and the forces in charge of the interactions between the edges of the tip and the sample would be at the origin of the dot formation.

The objective of the next experiments is to measure qualitatively and quantitatively the impact of the field enhancement in the nanopattern formation.

3.c. Influence of the Tip Electromagnetic Singularity in the Nanoprotrusion Formation. According to the experimental spatial periodicity of the fringes, the dot appears in the zone of maximal intensity, which seems to contradict observations in holography and most of the theoretical migration predictions of chromophores. Therefore, it is necessary to determinate if the photoinduced dot results mainly from an exaltation of the electromagnetic wave scattered by the tip. To validate this hypothesis, a series of experiments have been carried out. The first experiment consists of measuring the speed formation of the dot according to the polarization state although dots could be induced using p- and s-polarized actinic light.

3.c.1. Influence of the Incident Polarization. According to H'Dhili et al.,[25] who studied nanopatterns formation via intermittent or tapping scanning mode, we assume that the height of nanopattern can be considered as a snapshot of the field effect (FE). Thus, the polarization of the actinic light should affect the nanopattern formation. The reflection illumination mode, a Pt-coated tip, and a whisker tip were used for these experiments. For the same illumination dose (see previous section), the height of the nanoprotrusion was successively measured in the p and s states of polarization of the laser beam.

Results presented in Figure 7 indicate that whatever the equivalent dose of illumination for p- and s-polarized light (above or below the threshold, from 3.33 to 20 J cm^{-2}), no clear changes appear in the height of the photoinduced protusions. Moreover, the polarization do not appear to be dependent on the concentration of he copolymer as well as the solvent used for the experiments.

The reorganization of the chromophores when exposed to a p-polarized light does not seem to result from an exaltation of the electromagnetic wave at the apex of the metallic tip. To determine the role of the singularity electromagnetic wave, further experiments were carried out.

3.c.2. Influence of the Tip Material. Experimental conditions have been chosen in order to minimize the FE. According to the near field FE theory, when electromagnetic waves reach the apex of a sharp metallic tip, they induce several physical phenomena such as an increase of the charge density at the apex. If the density of charge is involved in the pattern formation, a semiconductor (e.g., silicon (Si)) or a dielectric tip (e.g., silicon nitride (Si_3N_4)) should not interact with the surface to induce the same protusions as the one obtained with a metallic tip (e.g., Si covered by Pt). The electromagnetic field exaltation induced by a semiconductor tip should be lower than the one induced by a metallic tip. The dielectric tip (low ϵ) should be considered like a negative referee for the test. All the tips have been used in the contact scan mode. The chosen zone of the sample is exposed for 30 s with a laser beam power about 8 mW in the reflection illumination configuration.

To illustrate the influence of the tip material, we performed a 2D simulation of the electromagnetic exaltation for different kinds of tips using the finite element method (FEM).[30,31] This methodology enables first to apprehend qualitatively the electromagnetic singularity for each kind of tips depending on their nature, the intensity distribution of the light source, and the angle of illumination of the tip. Second, those simulations are compared to the experimental results in order to correlate numerical and experimental observations. The efficiency of this method was demonstrated by Fikri et al.,[31] who proposed a complete model of ASNOM taking into account the realistic tip vibration

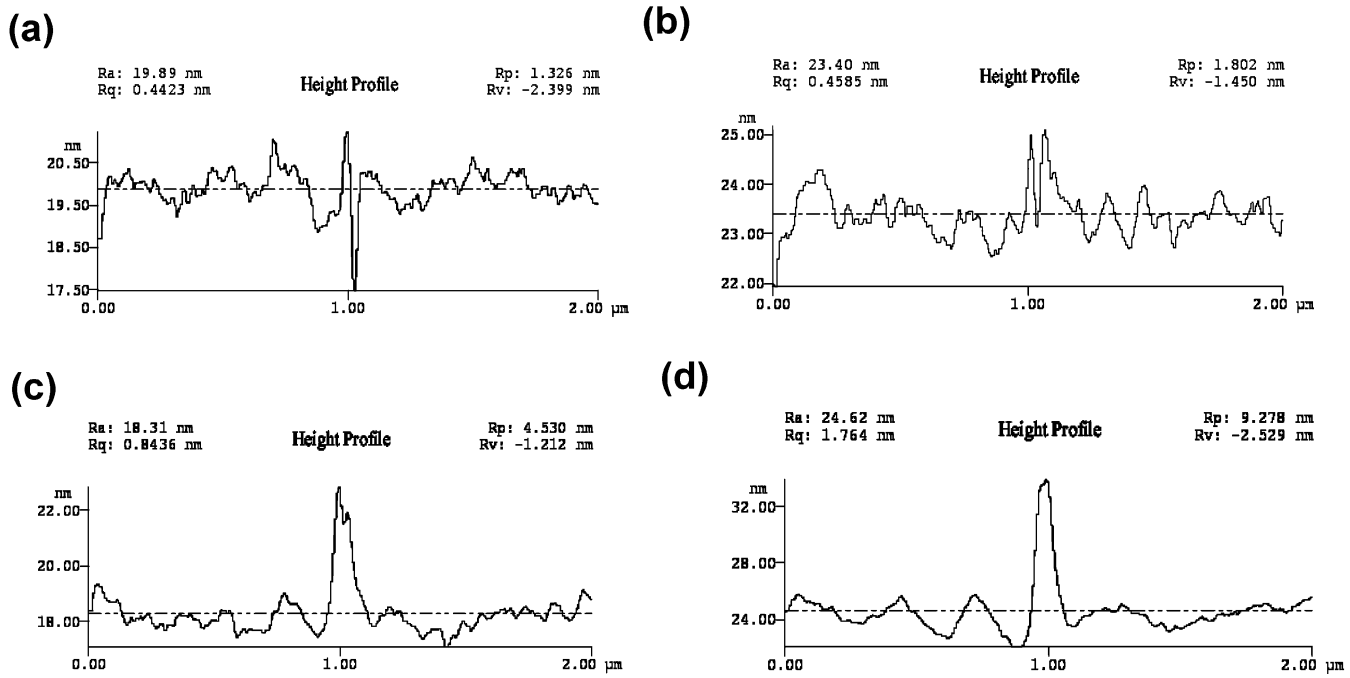

Figure 6. Effect of the illumination time on the nanopattern growth (height in nm). Parameters: power 2.2 mW; time of exposure: (a) 1, (b) 2, (c) 4, and (d) 10 s. This dynamism is observed in either ATR or reflection.

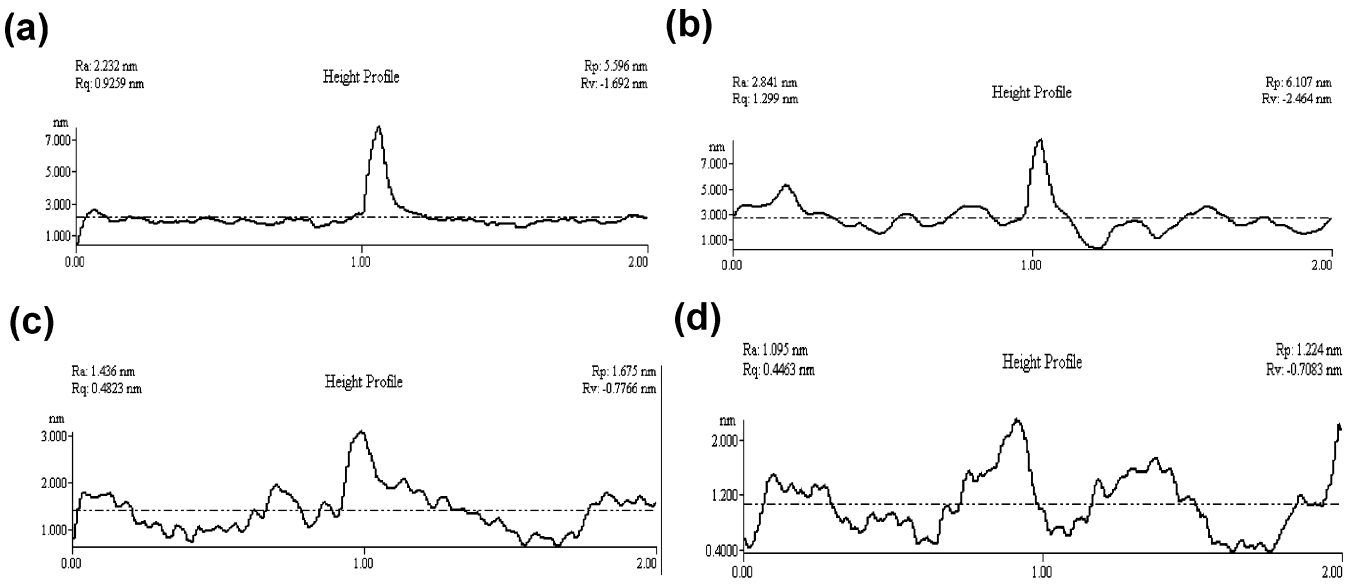

Figure 7. Influence of the polarization of the actinic light on the nanopattern formation: 0.2 mg of copolymer dissolved in 5 mL of THF, Csc 17 tip in reflection configuration. Power 5.9 mW; time of exposure 1 s for p polarization (A) and for s polarization (B). 0.1 mg of copolymer dissolved in 7 mL of MIBK, Csc 17 tip in reflection configuration. Power 0.035 mW; time of exposure 30 s for p polarization (C) and for s polarization (D).

and the lock-in detection; numerical results were in good agreement with the experimental ones.

The results of the 2D FEM simulations are presented in parts a and b of Figure 8 respectively for a Pt-coated Si tip and a Si tip. Calculations suggest that the electromagnetic field shows a radial confinement at the apex in both cases. Difference of the intensity scattered by the tip is due to the conductivity of the material (dielectric constant). Additional calculation (not shown here) has shown that dielectric tip does not present any confinement.

However, experimental results revealed a lack of differences between the nanopatterns induced by a metal or semiconductor probe. Figure 9 shows a photoinduced dot induced by a Si tip which displays the same properties as the nanopattern obtained when using a platinum probe. The relative large diameter of the protrusion is due to large aperture angle of the tip. Moreover, use of a dielectric tip (Si_3N_4) also leads to the formation of protusions (see Figure 10). This result appears to be in contradiction with the numerical simulations and with the field enhancement theory.

Another experiment has been carried out to evaluate the influence of the FE: it consists of applying experimental condition that decreases the FE and observing its consequences on the growth of nanopatterns. It is based on another method of illumination: the normal incidence one. This configuration is expected to minimize both the FE and the field confinement.

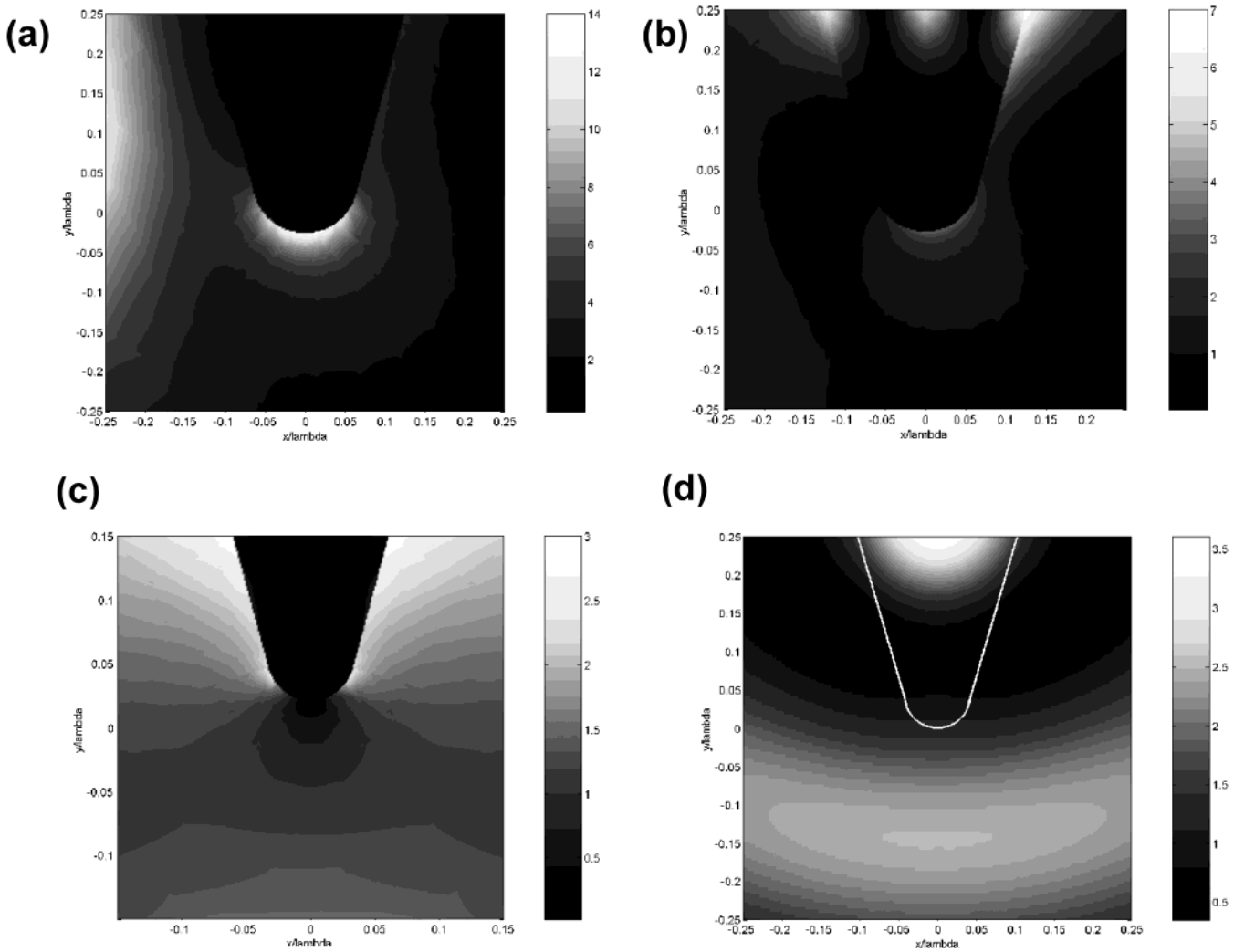

Figure 8. Simulations of the confinement of the electromagnetic wave by 2D FEM, The scale on the right indicates the value of exaltation (I/I_0, I_0 is the incident intensity). Dimensions scales are in nm/wavelength (e.g., for 0.1 read corresponds to 53.2 nm). In reflection mode for a TM polarization: (A) Si /Pt tip and (B) Si tip. For (A), we observe a field enhancement in the vicinity of the tip end. For (B) we observe a propagation of the light inside the silicon tip. In normal incidence mode for a Si tip in TM polarization (C) and for Si_3N_4 tip in TE polarization (D). For (c) and (d), there is no FE at the apex of the tip.

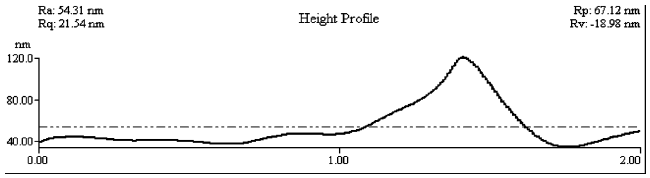

Figure 9. Profile of the nanopattern by modulation of the Si Csc11 tip deflection in reflection mode. Height 72 nm. Time of exposure is around 40 s, and the power of actinic light is 12 mW. Length scale is 2 μm.

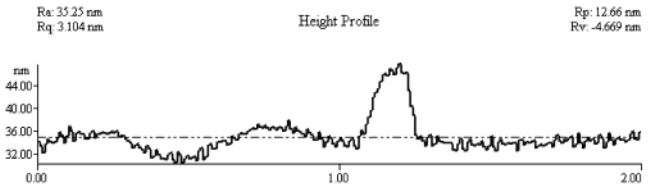

Figure 10. Profile of the nanopattern obtained by modulating the Si_3N_4 tip deflection in reflection mode. Height 12 nm. Time of exposure is around 50 s, and the power of actinic light is 0.035 mW. Length scale is 2 μm.

3.c.3. Normal Incidence Illumination Mode. The 2D FEM simulations allow us to determine an angle of illumination of the Si and Si_3N_4 tips for which the confinement field at the apex of the tip disappears (by comparison with a tip made of Pt). This result is only valid for an irradiation issued from a laser beam with a fundamental Gaussian mode. Therefore, it is important to note that this illumination mode corresponds to the normal incidence one (Figure 8c).

For the 2D FEM simulation, the electric field is incorporated into the 2D plane of the model. For the silicon tip, a confinement of the electromagnetic wave on the side of the tip is present with a weak intensity as well as a quasi-null confinement at the apex of the tip. In other words, this mode of illumination is chosen because of the electromagnetic exaltation that may be involved in the growth of the nanopattern is significantly decreased. This feature is also mentioned by Novotny et al., who advised against the use of a Gaussian mode in an analogue mode of illumination and recommended a high-order Hermite−Gaussian beam mode (in TM mode) to induce a field enhancement.[32] For this experiment, Si tips, Si_3N_4 dielectric tips, and Pt-coated tips were used. Let us remind that Si_3N_4 tips are considered as a negative referee. In addition, the experimental conditions (see Figure 2c) were far away from the conditions required to induce the electromagnetic singularity.

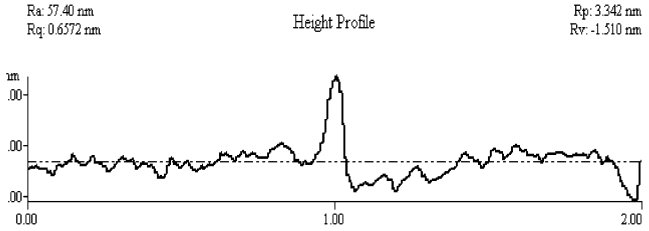

Figure 11. Profile of the nanopattern by modulation of the Si Csc11 tip deflection in normal incidence mode. Height 2.8 nm. Exposure time was around 30 s, and the power of actinic light is 5.6 mW. Length scale is 2 μm.

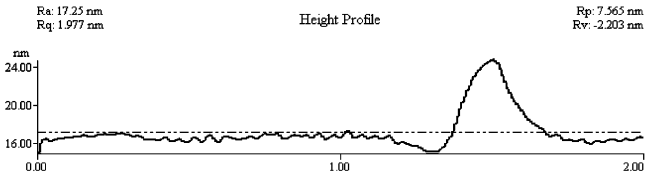

Figure 12. Profile of the nanopattern by modulation of the Si_3N_4 tip deflection in normal incidence mode. Height 7.5 nm. Exposure time is around 30 s, and the power of actinic light is 12 mW. Length scale is 2 μm.

Under these conditions, nanoprotusions were photoinduced whatever the tip material, as shown in Figures 11 and 12. Patterns are featured with heights of 2.8 and 7.1 nm for a semiconductor and a dielectric probe from the AFM profiles. Before discussing these results, it is necessary to determinate whether the nanopattern can be explained by the tridimensional reorganization of chromophores observed in far field.

3.c.4. Erasure and Repeatability of the Nanopattern Formation. Photochromic nature of the deposited film implies a reversible molecular rearrangement of the chromophores due to the azobenzene group. According to Bian et al., when the illumination power is higher than a specific value, the illumination of an azo polymer leads to a pattern shifted in phase (in comparison with the pattern usually obtained).[12] When the sample is irradiated under those conditions, an unerasable peak appears which can be induced by a possible bleaching process. A comparison between far field and near field is thus necessary to prove the similitude between those results and our observations under the tip. In other words, we must determinate whether the nanopattern photoinduced under the tip apex results from a process similar to the one described in far field.

The reflection illumination mode was here selected because it enables both the surface deformation in the vicinity of the metallic tip apex and the formation of interference fringes resulting from interactions between the actinic light and light reflected by the entire tip. The normal incidence illumination mode was also used to compare erasure properties of the reflection mode with an illumination mode minimizing the lightning rod effect. The photoinduced nanopattern obtained with different times of irradiation starting from 1 to 45 s (λ = 532 nm, P = 8 mW) can be optically erased by an exposition to the actinic light once the metallic tip is retracted. The erasure of the nanopattern required an energy dose more important that the one necessary to induce nanoprotusions. Writing and erasure processes can be repeated in the same zone without any change in the dynamics of the surface deformation. Thus, a rewritable process can be carried out in the same area. The same results in the vicinity of the tip are obtained with the normal incidence illumination mode. As this mode leads to a minimal electromagnetic singularity, the correlation between the topographic features observed using the normal incidence and reflection illumination modes shows that there is no induction of an irreversible peak.

As a conclusion of subsection 3.c, the results suggest that forces involved in the growth of the dot are not related to the electromagnetic exaltation of the tip. It has been demonstrated that the polarization does not influence the speed of formation of the nanoprotrusion whatever the energy dose used. Moreover, a nanopattern is observed whatever the tip material while a conductive material is required to exalt the electromagnetic wave. Combining a nonmetallic probe with an illumination mode avoiding radial confinement still gives rise to photoinduced nanopattern. If the electromagnetic field enhancement is involved in the process of the nanoprotrusion formation, the influence of this factor is minor. Therefore, azobenzene groups do not seem to represent an efficient snapshot of the electromagnetic field scattered by the probe although the dot growth is triggered by optical absorption (see subsection 3.a). Nanometric protrusions appear to be mainly issued from interaction forces that are not a tributary of the electromagnetic singularity.

Others experiments are presently being carried out to exalt the tip effect factor. They will be described in a following article. We have to recall that this interpretation only concerns protusions obtained in the contact scan mode experimental protocols. Previous results show that the interactions between the tip and the sample surface are issued from attractive forces different from the lightning rod effect. The next paragraph consists of apprehending the nature of the forces, allowing the adhesion and leading to the formation of the nanopattern.

3.d. Determination of Forces Involved in the Nanoprotrusion Formation. 3.d.1. Adhesion Forces. The objective of this subsection is to demonstrate that the forces implied in the nanopattern growth, which are different from those due to the electromagnetic singularity, can be adjusted in order to control the structure under the apex of the tip.

In all the previous experiences, the selected value of the set point is maintained constant: deflection of the scanmaster Z piezo (and consequently the involved forces) remains the same during the illumination step. For the next experiences, the set point is tuned as the sample is irradiated; thus, the distance between the tip apex and the sample is gradually increased or deceased. As the previous choice for the set point value corresponds to the limit of retraction of the Z piezo, the modification of this value should lead to a complete retraction of the piezo. Selected tips for this experiment are made of Si coated by Pt (metallic), Si (semiconductor), and Si_3N_4 (dielectric). Experimental configurations are analogues to the ones used for the normal incidence and reflection illumination modes. When irradiating the sample, modifications of the set point value do not lead to an immediate retraction of the Z piezo except when choosing directly arbitrary extreme set point values (−100 nN). The dynamics of this process reveals different topography obtained by varying the initial set point value before irradiation and by modulating this value during the exposure for a given illumination dose value. Topographic modifications are easily obtained.

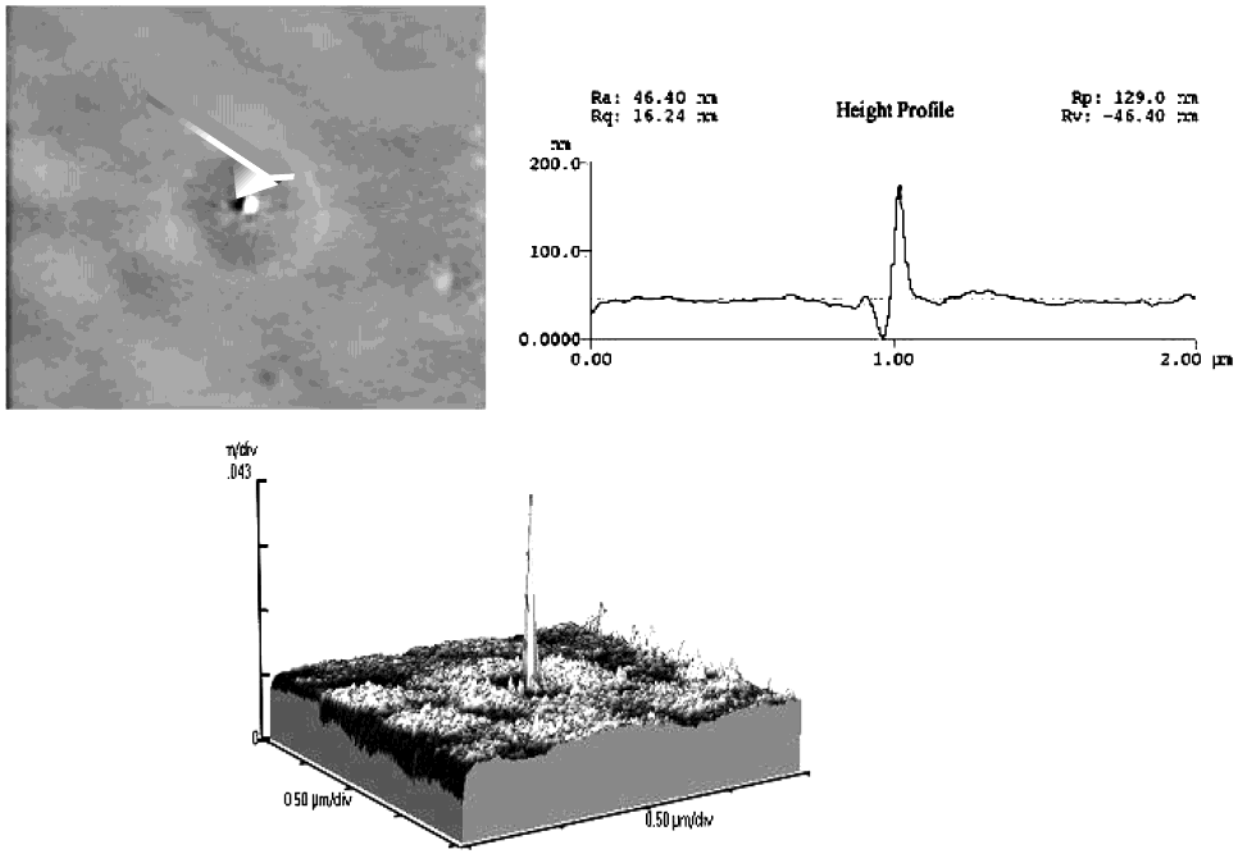

Figure 13. AFM image (2 μm × 2 μm), profile, and 3D view of a nanopattern induced by the modulation of a Si tip deflection in normal incidence mode. 3D representation of the cantilever and the AFM tip position onto the sample surface. Height of the nanoprotrusion is 120 nm, and depth of the hole is 26 nm. Length scale is 2 μm.

The use of Si- or Pt-coated tip, in reflection mode, leads to nanopatterns and gives rise in both cases easily to a dot formation. The dot presents features mentioned in previous subsection, including the optical erasure and the photoinduced nature of the process. Moreover, in normal incidence illumination configuration, it is also possible to obtain specific surface modulation identical to the one obtain with a fixed set point value even with a semiconductor or a dielectric tip.

Set point modulations like a fast Z piezo retraction can lead to singular protusions like the pattern in Figure 13. There is formation under the vicinity of a central hole having a depth of 26 nm and a peak of protrusion featuring a fwhm of 30 nm and a height of 100 nm. Thus, a near-field resolution of quasi $\lambda/18$ is obtained. Around the pattern, a ring is materialized; it results from the interference between the actinic light coming directly from the source and the one scattered by the tip.

These results suggest that the dot seems to come from an interaction between the edge of the tip apex and the surface of the copolymer. The dot of Figure 13 mainly corresponds to a lateral protuberance that adheres to the tip edge. Its height is amplified due to the drastic change of the set point value.

It is possible to observe a nanoprotrusion if the variation of the set point value enables a complete retraction of the Z piezo. Otherwise, a nanopattern with a depletion remaining at its summit is obtained. The dot height is controlled by the energy dose received and by the Z piezo retraction. These data tend to justify the influence of adhesion forces on the growth of nanoprotusions.

Consequently, we have to mention the list of the factors, other than optics, that could be involved in the nanopattern formation. When two solids are in contact, the molecular attraction strengths have an intensity which depends on nature of the molecular bindings ensuring the cohesion of the materials. These forces are responsible for the natural adhesion of the solids. This adhesion phenomenon results from molecular interactions like electrostatic forces and van der Waals forces.

As the electrostatic forces are long-range interaction forces they first attract the surface sample to the tip. When the two materials are close enough to each other, the van der Waals forces, which are shorter range and stronger than Coulombic forces, take over the electrostatic forces. If a permanent dipolar moment of DR1 molecules (for trans isomer) existed locally, it would apply an electric field on the material forming the tip. If the tip had a dipolar moment, Keesom forces would be induced and an attractive field would appear. If the molecules of the probe did not have any polar moment, one could be induced by Debye forces. Dispersion properties (London forces), due to the electron fluctuations around atoms, can also lead to the instantaneous interaction from the dielectric probe and the polar copolymer.

Another kind of attractive force can be mainly involved in the growth of nanoprotusion: the capillary forces. These kinds of forces are mainly due to thin water film that is always present at the surface of a sample plunged in the ambient humid air (33%). Near the surface, the tip apex is comparable to a microswitch which acts like a core of condensation. If the radius of curvature of the microswitch is lower than a certain

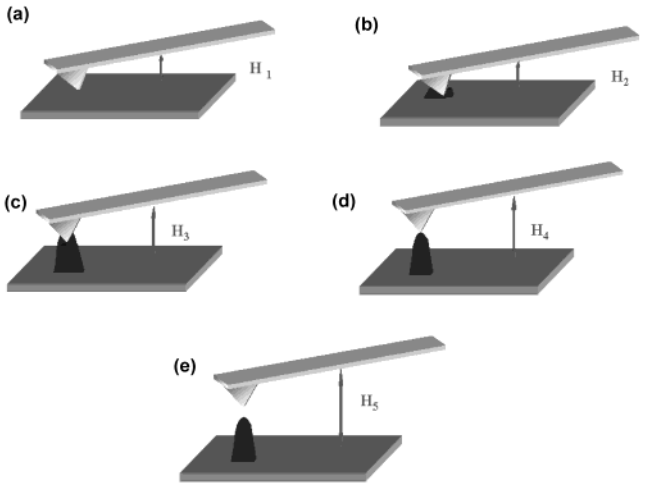

Figure 14. Interpretation of the nanopattern formation and growth. (a) represents the initial position of the tip onto the surface sample. When the illumination phase is triggered, protuberances appear first on the side of the tip as it is shown in (b). (c) and (d) show a tridimensional reorganization of the chromophores which leads to an increase of the distant H between the unexposed surface sample and the apex of the tip in order to maintain the value applied to the set point. (e) shows a complete retraction of the Z piezo.

value, a meniscus is formed. It results in an attractive force from gravitational capillarity between the tip apex and the sample. Experiments in progress are carried out to determine the influence of this force by placing the sample in a dry atmosphere (N_2).

The mathematical theory of Gaididei et al.[7] demonstrates the importance of intermolecular interactions (e.g., van der Waals) in the reorganization of chromophores containing an azobenzene group when irradiating. This approach tends to corroborate our experimental result. The migration of the DR1 in our experiment seems to be perturbed by the physical presence of a material close enough to the surface to generate adhesion forces via polarization forces.

A beginning explication for the global mechanism can be apprehended from all results collected.

The value corresponding to the limit of retraction of the Z piezo makes the tip interact with the irradiated sample only via its apex (Figure 14a). Then, redistribution of chromophores tends to adhere to the edges of the apex that present an important surface of contact. This process gives rise to lateral protuberances and thus contributes to the formation of a local depletion (Figure 14b). According to the energy dose, these protuberances tend to become bigger as the adhesion forces enhance (Figure 14c).

Therefore, if the volume occupied by those lateral modifications increases, the distant from the apex to the surface tends to decrease. In the case of a fixed set point value, the accumulation of matter tends to modify the deflection value of the cantilever. Therefore, the feedback loop of the scanmaster induces an increase of the distance tip−unexposed sample surface to maintain the set point value constant. When the reorganization of chromophores fills the local depletion and constitutes a dot shape, the apex of the tip cannot be any longer driven into the depletion formed by the lateral protuberances (Figure 14d). Therefore, interactions of the sample with the edge of the tip decrease drastically. If the tip presents a small radius of curvature, the adhesion forces could not avoid the complete retraction of the Z piezo (feedback loop cannot adjust the deflection to approach the tip to the surface quickly and sufficiently, Figure 14e). This mechanism can be correlated with the results obtained once the set point value is modulated inducing a fast retraction of the Z piezo of the scanmaster. The height of the nanoprotusions suggests that the reorganization of chromophores inducing a "stable" nanoprotrusion does not appear immediately. Adhesion forces are first triggered and determine a "preshape".

3.d.2. Role of the Solvent. The efficiency of the chromophores migration depends on the free volume necessary to allow the trans−cis isomerization of the azobenzene group. Therefore, the residual solvent present in the sample should be involved in this process.

Several experimental observations seem to correlate with this hypothesis. For some experiments, the MIBK (see subsection 2.a) has been replaced by tetrahydrofuran (THF). This solvent is chosen because of its high volatility in order to significantly decrease the thermal treatment time. However, when operating under a controlled atmosphere (with a weak hygroscopy) during a prolonged time, no modification of the topography can be photoinduced whatever the illumination mode. Then, introduction of another identical sample, which has not been previously brought in a dry atmosphere, permits to feature nanoprotrusion according to the previous experimental protocols.

Moreover, 3 or 4 month old samples do not easily allow induction of protusions if they are maintained in normal environmental conditions. These observations lead to the conclusion that the solvent acts as a plasticizer for the copolymer.

MIBK is a strong solvent for copolymer. Its high dielectric constant (13.1) leads to use MIBK as good polar solvent, and its moderate evaporation rate enables the photoisomerization. Chromophores can reorganized either in diads or triads by electrostatic and van der Waals interactions.[7,13,14] These tridimensional reconfigurations of chromophores prevent DR1 molecules to reorient themselves and increase the global rigidity/stability of the sample. Consequently, the isomerization process should require an energy dose higher than the theoretical energy necessary to induce this feature for a single DR1 molecule. However, the copolymer is dissolved in a polar solvent. By analogy to Zucolotto et al.'s work assessing the role of water molecules in layer by layer (LBL) films of azobenzene, MIBK is going to disrupt this rigidity by intercalating itself between DR1 molecule, thus reducing the interaction between NLO chromophores.[33] Therefore, chromophores dispose of an important free volume, which is sufficient to enable the trans−cis isomerization (isomerization process requires a minimal volume of 0.2 nm^3).[32] To conclude, the MIBK polar solvent acts as a plasticizer that favors the migration and reorganization of chromophores.

3.d.3. Role of the Matrix. The MMA polymer constitutes an inert matrix (to the $\lambda = 532$ nm emission wavelength of the laser beam). During the illumination phase, MMA is pushed and/or pulled by the chromophores that are covalently bounded to the matrix. The nanoprotrusion should induce mechanical stress in the matrix and thus deformation (including a mechanism such as torsion compression and elongation of the MMA unit). However, the matrix presents a high tensile strength (55−80 MN/m^2), a high tensile modulus (2−3 G/m^2), and a low elongation at break (<10%). Those

physical characteristics and experimental results show that the surface migration and reorganization which can be erased and reinduced are not due to a cleavage of the thermoplastics MMA units.

In addition to the hypothesis of mechanism related in the previous subsection, we assume that the dot shape of the nanopattern results from a competition between the adhesion forces between the tip apex and the sample surface and the intrinsic mechanical forces. If the strength of adhesion forces applied on the surface is smaller than the yield strength of MMA units, the matrix would prevent migration of the lateral chain containing chromophores and support a stable tridimensional reorganization of azobenzenes. Tribological features (e.g., elastic strain, viscoelasticity or plasticity, speed of rupture of the matrix) determine the adherence forces. These forces can greatly vary according not only to the mechanical behaviors of the copolymer but also to the environmental parameters such as the presence of contaminants, the temperature, and hygroscopy. Further experiments need to be carried out to determine accurately the complex mechanism of the nanopattern formation.

4. Conclusion

Photoinduced nanoprotusions present main properties such as a stable surface modulation, an optically reversible and fast process according to the local illumination dose. These properties are comparable with the dynamic and reorganization of chromophores when they form the surface relief gratings (SRG) in far field. The presence of the tip on the surface of the film seems to mechanically pertubate the rearrangement of the chromophores. This modification leads to a nanometric dot.

As a result, we have introduced a new method of nanolithography based on the mutual use of the AFM contact scanning mode and the normal incidence illumination mode. The contact-scanning mode has been chosen during these experiments to allow more important and longer interactions between the probe apex and the copolymer sample surface than the other scan modes (e.g., intermittent contact mode and noncontact mode). Consequently, this mode enables to deepen research on interaction forces involved in the dot formation. Moreover, this mode enables to fabricate easily nanoprotusions so it facilitate a better search for their properties.

In this scanning mode, it has been demonstrated that the presence of confined electromagnetic waves below the tip does not significantly influence the growth speed of the nanoprotusion. In this case, adhesion forces are mainly involved in the formation of the protusion. These forces can have variable origins such as the polarization forces. All of them contributes to generate an attractive force which links and maintains the surface sample to the edges of the tip apex regardless to the tip material. The solvent (plasticizer) makes migration easier by preventing dyad and/or triad formation and enables trans−cis isomerization. Moreover, the dot height can be amplified by the modulation of the probe deflection while irradiating.

Tips are chosen with the appropriate radius of curvature (presenting a surface of contact more or less important at its apex) according to the lateral and height dimensions required for the dots. Even if the adhesion force is in charge of this growth, it cannot explain the initial migration and reorganization of the chromophores.

This phenomenon has an optical origin: the surface required to be irradiated from a laser source which emission wavelength is included in the absorption band of the DR1. The simplicity of this process can lead this kind of nanochemistry to be widely experimented. Besides, the numerous parameters and features observed justify the interest in the polymer containing azobenzene groups and their applications in nanophotolithography. Many tests are still required to complete our knowledge on the phenomenon of spatial reorganization and to affirm their validity in the industry, in particular their time evolutions as a function of external parameters like the pressure, the temperature, the presence of oxygen, or hygrometry. Currently, experiments carried out in our laboratory are focusing in exalting the electromagnetic singularity to photoinduce nanopattern with other tribologic features.

Acknowledgment. The authors thank the Department of Photochemistry (Université de Haute Alsace-Mulhouse) for valuable discussions.

References and Notes

(1) Hartley, G. S. *Nature (London)* **1937**, *140*, 281.
(2) Rochon, P.; Batalla, E.; Natansohn, A. *Appl. Phys. Lett.* **1995**, *66*, 136.
(3) Kim, D. Y.; Tripathy, S.; Li, K.; Kumar, J. *Appl. Phys. Lett.* **1995**, *66*, 1166.
(4) Sumaru, K.; Yamanaka, T.; Fukuda, T.; Matsuda, H. *Appl. Phys. Lett.* **1999**, *75*, 1878.
(5) Sumaru, K.; Fukuda, T.; Kimura, T.; Matsuda, H.; Yamanaka, T. *J. Appl. Phys.* **2002**, *291*, 3421.
(6) Chen, P. C.; Chieh, Y. C. *J. Mol. Struct.* **2003**, *624*, 191.
(7) Gaididei, Y. B.; Christiansen, P. L.; Ramanujam, P. S. *Appl. Phys. B* **2002**, *74*, 139.
(8) Pedersen, T. G.; Johansen, P. M.; Holme, N. C. R.; Ramanujam, P. S. *Phys. Rev. Lett.* **1998**, *80*, 89.
(9) Lefin, P.; Fiorini, C.; Nunzi, J. M. *Opt. Mater.* **1998**, *9*, 323.
(10) Barrett, C. J.; Natansohn, A.; Rochon, P. *J. Phys. Chem.* **1996**, *100*, 8836.
(11) Kumar, J.; Li, L.; Jiang, X.; Kim, D.-Y.; Lee, T. S.; Tripathy, S. *Appl. Phys. Lett.* **1998**, *72*, 2096.
(12) Bian, S.; Williams, J. M.; Kim, D. Y.; Li, L.; Balasubramanian, S.; Kumar, J.; Tripathy, S. *J. Appl. Phys.* **1999**, *86*, 4498.
(13) Choi, D. H. *Bull. Korean Chem. Soc.* **1999**, *20*, 1186.
(14) Choi, D. H. *Bull. Korean Chem. Soc.* **1999**, *20*, 1010.
(15) Buffeteau, T.; Lagugné-Larbathe, T. F.; Pézolet, M.; Sourisseau, C. *Macromolecules* **1998**, *31*, 7312.
(16) Lagugné-Labarthet, F.; Freiberg, S.; Pellerin, C.; Pézolet, M.; Natansohn, A.; Rochon, P. *Macromolecules* **2000**, *33*, 6815.
(17) Lagugné-Labarthet, F.; Buffeteau, T.; Sourisseau, C. *Phys. Chem. Chem. Phys.* **2002**, *4*, 4020.
(18) Cvilinski, J.; Tajbakhash, A. R.; Ternjev, E. M. *EPJ* **2002**, *9*, 427.
(19) Serak, S.; Kovalek, A.; Agashkov, A.; Gleeson, H. F.; Watson, S. J.; Reshentyak, V.; Yaroschuk, O. *Opt. Commun.* **2001**, *187*, 235.
(20) Brozozowski, L.; Sargent, E. H. *J. Mater. Sci.: Mater. Electron.* **2001**, *12*, 483.
(21) *Champ proche optique: Théorie et Applications*; Courjon, D., Bainier, C., Eds.; *Springer collection technique et scientifique des télécommunications*, France, 2001.
(22) Bachelot, R.; H'Dhili, F.; Barchiesi, D.; Lerondel, G; Fikri, R.; Royer, P. Landraud, N.; Peretti, J.; Chaput, F.; Lampel, G.; Boilot, J. P.; Lahli, K. *J. Appl. Phys.* **2003**, *94*, 2060.
(23) Bohn, J. L.; Nesbitt, D. J.; Gallager, A. *J. Opt. Soc. Am. A* **2001**, *18*, 2998.
(24) Larsen, R. E.; Methiu, H. *J. Chem. Phys.* **2001**, *114*, 6851.
(25) H'Dhili, F.; Bachelot, R.; Lerondel, G.; Barchiesi, D.; Royer, P. *Appl. Phys. Lett.* **2001**, *79*, 4019.
(26) Lee, H. W.; Kim, Y. M.; Jeon, D. J.; Kim, E.; Kim, J.; Park, K. *Opt. Mater.* **2002**, *21*, 289.
(27) Iwata, F.; Kobayashi, K.; Sasaki, A.; Kawata, Y.; Egami, C.; Sugihara, O.; Tuchimori, M.; Watanabe, O. *Nanotechnology* **2002**, *13*, 138.
(28) Patanè, S.; Arena, A.; Allegrini, M.; Andreozzi, L.; Faetti, M.;

Giordano, M. *Opt. Commun.* **2002**, *210*, 37.
(29) Smith, M. A. G.; Mitchelland, G. R.; O'Leary, S. V. *J. Opt. A: Pure Appl. Opt.* **2002**, *4*, 474.
(30) Fikri, R.; Barchiesi, D.; H'Dhili, F.; Bachelot, R.; Vial, A.; Royer, P. *Opt. Commun.* **2003**, *221*, 13.
(31) Fikri, R.; Grosges, T.; Barchiesi, D. *Opt. Lett.* **2003**, *28*, No. 22.
(32) Novotny, L.; Sanchèz, E.; Xie, X. S. *Ultramicroscopy* **1998**, *71*, 21.
(33) Zucolotto, V.; Mendonça, C. R.; dos Santos, D. S., Jr.; Balogh, D. T.; Zilio, S. C.; Oliviera, O. N., Jr.; Constantino, C. J. L.; Arcoa, R. F. *Polymer* **2002**, *43*, 4645.

MA035437G